MOLECULAR AND CELLULAR BIOLOGY, Apr. 2002, p. 2769–2776 Vol. 22, No. 8
0270-7306/02/$04.00+0 DOI: 10.1128/MCB.22.8.2769–2776.2002

Hydrocephalus, Situs Inversus, Chronic Sinusitis, and Male Infertility in DNA Polymerase λ-Deficient Mice: Possible Implication for the Pathogenesis of Immotile Cilia Syndrome

Yosuke Kobayashi,[1] Miho Watanabe,[2] Yuki Okada,[3,4] Hirofumi Sawa,[3,4] Hiroyuki Takai,[1] Makoto Nakanishi,[5] Yosuke Kawase,[2] Hiroshi Suzuki,[2] Kazuo Nagashima,[3,4] Kyoji Ikeda,[1] and Noboru Motoyama[1]*

Department of Geriatric Research, National Institute for Longevity Sciences, Obu, Aichi 474-8522,[1] Pharmaceutical Technology Laboratory, Chugai Pharmaceutical Co., Ltd., Gotemba, Shizuoka 412-8513,[2] Laboratory of Molecular and Cellular Pathology, Hokkaido University Graduate School of Medicine,[3] and CREST, JST,[4] Sapporo 060-8638, and Department of Biochemistry, Nagoya City University Medical School, Nagoya 467-8601, Japan[5]

Received 28 November 2001/Returned for modification 14 January 2002/Accepted 25 January 2002

A growing number of DNA polymerases have been identified, although their physiological function and relation to human disease remain mostly unknown. DNA polymerase λ (Pol λ; also known as Pol β2) has recently been identified as a member of the X family of DNA polymerases and shares 32% amino acid sequence identity with DNA Pol β within the polymerase domain. With the use of homologous recombination, we generated *Pol* $\lambda^{-/-}$ mice. *Pol* $\lambda^{-/-}$ mice develop hydrocephalus with marked dilation of the lateral ventricles and exhibit a high rate of mortality after birth, although embryonic development appears normal. *Pol* $\lambda^{-/-}$ mice also show situs inversus totalis and chronic suppurative sinusitis. The surviving male, but not female, *Pol* $\lambda^{-/-}$ mice are sterile as a result of spermatozoal immobility. Microinjection of sperm from male *Pol* $\lambda^{-/-}$ mice into oocytes gives rise to normal offspring, suggesting that the meiotic process is not impaired. Ultrastructural analysis reveals that inner dynein arms of cilia from both the ependymal cell layer and respiratory epithelium are defective, which may underlie the pathogenesis of hydrocephalus, situs inversus totalis, chronic sinusitis, and male infertility. Sensitivity of *Pol* $\lambda^{-/-}$ cells to various kinds of DNA damage is indistinguishable from that of *Pol* $\lambda^{+/+}$ cells. Collectively, *Pol* $\lambda^{-/-}$ mice may provide a useful model for clarifying the pathogenesis of immotile cilia syndrome.

DNA polymerases play an essential role in the maintenance of genome integrity during DNA replication, DNA repair, DNA recombination, and meiotic processes and also in checkpoint function in response to DNA damage. Recently, various DNA polymerases have been identified (7, 12, 14).

DNA polymerase β (Pol β) has been implicated in base excision repair (BER) in mammalian cells (5, 22, 23, 27, 29) and consists of two catalytic domains: a C-terminal domain (31 kDa) that possesses DNA polymerase activity (25) and an N-terminal domain (8 kDa) that binds a single-stranded DNA and exhibits 5′-deoxyribose phosphodiesterase (lyase) activity (18). Pol β possesses both polymerase and lyase activities, suggesting that it functions in short-patch BER by catalyzing the removal of a 5′-deoxyribose phosphate and filling the resultant single-nucleotide gap (30). It has been reported that DNA Pol δ and Pol ε are involved in a gap-filling step during long-patch BER (8, 19) because these enzymes are known to be stimulated by PCNA and are proficient in a reconstituted long-patch BER system (5). Pol β, too, has been implicated in long-patch BER (5, 27), meiosis (26), and nucleotide excision repair (13, 24). Although Pol β is the main DNA polymerase that is involved in short-patch BER of lesions generated by monofunctional alkylating agents such as methylmethane sulfonate (MMS) (30), certain short-patch BERs have been observed in the absence of Pol β (6, 31). These observations suggest that some other DNA polymerase(s) functions in BER processes.

We and others have recently identified DNA Pol λ (2, 10), also known as Pol β2 (21), which belongs to the Pol X family. Its C-terminal polymerase domain shares 32% amino acid identity with the corresponding region of Pol β. Pol λ has an additional 230-amino-acid region with a BRCA1-containing carboxy-terminal (BRCT) motif at the N-terminal region. The BRCT domain is found in DNA repair and cell cycle checkpoint proteins, including p53BP1, Rad9, Xrcc1, Rad4, Ect2, REV1, Crb2, RAP1, terminal deoxyribonucleotide transferase, and three eukaryotic DNA ligases (3, 4). Recently, Garcia-Diaz et al. reported that Pol λ has a 5′-deoxyribose-5-phosphate lyase activity and a strand-displacement synthesis activity on gapped DNA substrates (9), suggesting that Pol λ participates in short- and long-patch BER. Although Pol λ is detected in several tissues, it is abundantly expressed in pachytene spermatocytes of the testis and in the ovary (10, 21), suggesting that Pol λ is involved in meiotic cell division.

To clarify the physiological role(s) of Pol λ in vivo, we have generated mice as well as cells lacking Pol λ by using gene targeting with embryonic stem (ES) cells. Mice lacking Pol λ exhibit hydrocephalus, a high rate of mortality after birth, situs inversus totalis, chronic sinusitis, and male infertility due to immotility of sperm. Consistent with these phenotypes, electron microscopical analysis reveals a defect of inner dynein

* Corresponding author. Mailing address: Department of Geriatric Research, National Institute for Longevity Sciences, 36-3 Gengo, Morioka, Obu, Aichi 474-8522, Japan. Phone: 81 562-44-5651, ext. 826. Fax: 81 562-44-6595. E-mail: motoyama@nils.go.jp.

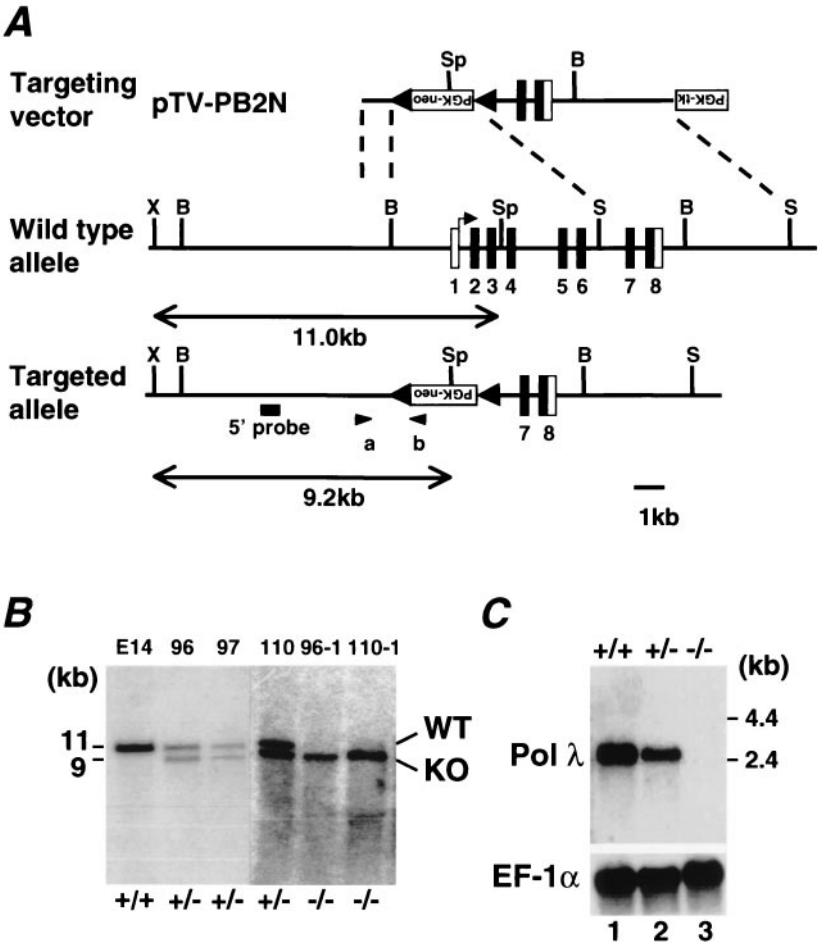

FIG. 1. Targeted disruption of the mouse *Pol* λ gene. (A) Structure of the targeting vector (pVT-PB2N), a restriction map of the mouse *Pol* λ locus, and structure of the targeted locus after homologous recombination. The coding and noncoding exons are numbered and depicted by closed and open boxes, respectively. The mutated *Pol* λ allele was detected by PCR with a pair of primers (a and b) indicated by arrowheads, and its presence was confirmed by Southern blot analysis with a 5′ probe indicated by the solid line. The expected sizes of the *Xba*I (X)-*Spe*I (Sp) fragments that hybridize with the probe on Southern analysis are indicated for wild-type (11.0-kb) and mutant *Pol* λ (9.2-kb) alleles. B, *Bam*HI; S, *Sac*I. (B) Southern blot analysis with the 5′ probe of *Xba*I- and *Spe*I-digested genomic DNA from wild-type (lane 1), targeted heterozygous ES clones 96, 97, and 110 (lanes 2, 3, and 4) and homozygous ES clones 96-1 and 110-1 (lanes 5 and 6). The 11.0- and 9.2-kb fragments corresponding to the wild-type (WT) and mutated (KO) alleles, respectively, are indicated. (C) Northern blot analysis of polyadenylated RNA from the testis of wild-type (*Pol* $\lambda^{+/+}$), *Pol* $\lambda^{+/-}$, and *Pol* $\lambda^{-/-}$ animals with *Pol* λ cDNA (top) and EF-1α cDNA (control) (bottom) probes. The signal intensity of *Pol* λ mRNA in *Pol* $\lambda^{+/-}$ testis was reduced approximately 50% compared with that in wild-type testis; no *Pol* λ mRNA was detected in the *Pol* $\lambda^{-/-}$ testis.

arms in the cilia from ependymal cells and respiratory epithelium of *Pol* $\lambda^{-/-}$ mice, which may account for the phenotypes.

MATERIALS AND METHODS

Construction of the *Pol* λ targeting vector. The mouse *Pol* λ gene was isolated by screening a mouse 129/Sv Lambda FIX II genomic library (Stratagene) with mouse *Pol* λ cDNA as a probe. A 15-kb phage clone containing exons 1 to 8 of the *Pol* λ gene was subcloned into the pBluescript II SK(+) vector (Stratagene). The targeting vector, pTV-PB2N, was designed to delete a 6.4-kb genomic fragment containing exons 1 to 6 and to replace it with a neomycin resistance (*neo*) gene that was under the control of the mouse phosphoglycerol kinase 1 (PGK1) gene promoter and linked to the PGK1 poly(A) sequence (20); this gene construct (PGK-*neo*) was flanked by *loxP* sequences to create a *lox-neo* cassette and placed in the orientation opposite to that of *Pol* λ gene transcription. The targeting vector contained 1.0- and 6.0-kb regions of homology upstream and downstream, respectively, of the *lox-neo* cassette, with the PGK-thymidine kinase gene (32) at its 3′-most end.

Homologous recombination and generation of germ line chimeras. The *Not*I-linearized targeting vector was introduced by electroporation into E14 ES cells with Gene Pulser (two pulses of 0.3 kV and 125 μF; Bio-Rad). Cells were subsequently cultured for 7 days in the presence of G418 (0.3 mg/ml) and 2 μM ganciclovir. Correctly targeted ES clones were identified by PCR with a pair of primers (Fig. 1A) that are specific to the *Pol* λ gene-flanking sequence of the targeting construct (5′-CCCGAATGGTGCCTTCTTTCCTAA-3′) and the PGK-*neo* cassette (5′-GGGTGGGGTGGGATTAGATAAATG-3′), respectively, and were confirmed by Southern blot analysis. Three ES cell lines heterozygous for the disrupted allele were microinjected into C57BL/6 blastocysts to generate chimeras (17). Chimeric males from three independent clones (designated 96, 97, and 110) passed the mutant allele to offspring, and the animals from all lines showed identical phenotypes. All mice were maintained in a specific pathogen-free animal facility at Chugai Pharmaceutical Co. The experimental protocol was approved by the animal studies committees of the National Institute for Longevity Sciences, Chugai Pharmaceutical Co., and Hokkaido University Graduate School of Medicine.

Tissue preparation and microscopic analysis. For light microscopic examination, tissues were fixed with 4% paraformaldehyde in phosphate-buffered saline and embedded in paraffin. For examination of sinusitis, tissues were macerated with 5% trichloroacetic acid for 2 days after fixation. Sections (6 μm in thickness) were prepared at multiple levels and alternately stained with hematoxylin-eosin

or subjected to terminal deoxynucleotidyltransferase-mediated dUTP nick end labeling analysis (11). For detailed analysis of hydrocephalus, approximately 300 serial sections (6 to 10 μm) were prepared from the interventricular foramen to the fourth ventricle of each mouse. The testis was fixed with Bouin's solution and stained with both hematoxylin-eosin and periodic acid-Schiff solution. For ultrastructural analysis, tissues were fixed with 2% glutaraldehyde, exposed to 1% osmium tetroxide, and transferred onto an embedding material, Epon 812 (TAAB, Berkshire, United Kingdom). Ultrathin sections were stained with both uranyl acetate and lead citrate and examined with an electron microscope (H-800; Hitachi).

Morphological and functional analysis of spermatozoa. Motility of the spermatozoa from the cauda epididymis was analyzed using an IVOS sperm analyzer (Hamilton). Sperm morphology was assessed by a sperm smear, and the number of abnormalities was evaluated. To analyze whether the nuclei of immotile sperm contribute to fertilization and subsequent embryonic development, intracytoplasmic sperm injection was performed, as described previously (16). Fertilized eggs were cultured up to the two-cell stage and transferred to recipient animals on day 0.5 of pseudopregnancy.

Evaluation of sensitivity to DNA damage. The sensitivity of *Pol* $\lambda^{-/-}$ ES cells to DNA-damaging agents and X-ray and UV irradiation was determined by measuring their colony-forming ability. Twenty-four hours after being plated onto gelatinized 6-well plates, *Pol* $\lambda^{+/+}$ and *Pol* $\lambda^{-/-}$ ES cells were exposed to hydrogen peroxide (H_2O_2), MMS for 1 h, X-rays, or UV irradiation (UVC radiation at 254 nm). For UV irradiation, the medium was aspirated prior to exposure. Cells were grown for 7 days, fixed with methanol, and stained with Giemsa solution, and the number of colonies was counted.

RESULTS

Disruption of the *Pol* λ gene. ES cells and mice with disrupted *Pol* λ alleles were produced by homologous recombination. Exons 1 to 6 of the *Pol* λ gene, which include the translation initiation site and coding sequences corresponding to the BRCT motif and half of the polymerase X domain, were replaced by a neomycin resistance (PGK-*neo*) gene (Fig. 1A). Three independent clones were identified as correctly targeted by PCR analysis and confirmed by Southern blot analysis (Fig. 1B). *Pol* $\lambda^{-/-}$ ES clones were generated by cultivating heterozygous ES clones in the medium containing a high concentration of G418 (3 mM), and the genotype of surviving clones was confirmed by Southern blot analysis (Fig. 1B). All of these heterozygous clones transmitted the mutant *Pol* λ allele through the germ line, and *Pol* $\lambda^{-/-}$ animals from all lines exhibited identical phenotypes. The presence of the null allele in these lines was demonstrated by Northern blot analysis (Fig. 1C).

Pol $\lambda^{-/-}$ mice exhibit hydrocephalus, situs inversus, and chronic sinusitis. *Pol* $\lambda^{-/-}$ mice showed a high rate of mortality after birth. About half of the *Pol* $\lambda^{-/-}$ mice died by 3 weeks of age (*Pol* $\lambda^{+/+}$/*Pol* $\lambda^{+/-}$/*Pol* $\lambda^{-/-}$ = 157/341/91 at 3 weeks) and about 70% died by 9 weeks (Fig. 2A). Pol λ does not seem to be essential for embryogenesis, since wild-type, heterozygous, and homozygous mutant mice were observed at the expected Mendelian ratio at embryonic day 18.5 (E18.5) (19:49:26).

Although newborn *Pol* $\lambda^{-/-}$ mice were normal in gross appearance at birth, they began to exhibit enlarged and dome-shaped heads, reminiscent of hydrocephalus, by 2 to 4 weeks of age (Fig. 2B). Mice with hydrocephalus also exhibited marked growth retardation (Fig. 2C). Macroscopically, the lateral ventricles were greatly dilated and the third ventricle was moderately enlarged, with marked thinning of the cerebral cortices (Fig. 2D and E). In addition, 5 of these 26 *Pol* $\lambda^{-/-}$ embryos showed situs inversus totalis (Fig. 2F).

To determine the age of onset of hydrocephalus in *Pol* $\lambda^{-/-}$ mice, histological analysis with serial sectioning from the interventricular foramen to the fourth ventricle of the brains of *Pol* $\lambda^{-/-}$ mice was performed from E10.5 through 9 weeks after birth. Microscopically, no evidence of dilatation of the lateral ventricle was observed between E10.5 and E18.5 (data not shown). Terminal deoxynucleotidyltransferase-mediated dUTP nick end labeling analysis revealed that the number of apoptotic cells in the brains of *Pol* $\lambda^{-/-}$ embryos was not distinguishable from that of wild-type littermates (data not shown). A slight enlargement of the lateral ventricles was initially observed in a small number of *Pol* $\lambda^{-/-}$ pups at postnatal day 1, whereas cortical neuronal development appeared normal (data not shown). At 4 weeks after birth, severe dilatation of the lateral ventricles with ependymal hyperplasia of the third ventricle and the cerebral aqueduct was found in some *Pol* $\lambda^{-/-}$ mice, although complete obstruction in the cerebrospinal fluid pathway was not recognized. No gross developmental anomaly was observed in the central nervous systems of *Pol* $\lambda^{-/-}$ mice, including the hippocampus, thalamus, midbrain, cerebellum, and medulla, although these structures were compressed due to the enlarged lateral ventricles. Thus, it is likely that *Pol* $\lambda^{-/-}$ mice develop hydrocephalus within the first few days after birth.

The presence of hydrocephalus and situs inversus totalis in *Pol* $\lambda^{-/-}$ mice reminded us of immotile cilia syndrome, due to abnormal structure and function of cilia. We therefore performed a histological analysis of the paranasal sinuses. As shown in Fig. 3A through C, *Pol* $\lambda^{-/-}$ mice developed chronic suppurative sinusitis with accumulation of polymorphonuclear leukocytes in the nasal cavity and inflammatory cell infiltration, mainly composed of plasma cells and angiogenesis in the submucosal regions of the tunica mucosa olfactoria (Fig. 3C). Furthermore, ultrastructural analysis revealed that the cilia from the respiratory epithelium and ependymal cell layer of *Pol* $\lambda^{-/-}$ mice lacked inner dynein arms (Fig. 3D and E).

Infertility in male Pol $\lambda^{-/-}$ mice. Infertility due to the defective movement of spermatozoa is a characteristic feature of immotile cilia syndrome. Since Pol λ is highly expressed in the testis, especially in late pachytene spermatocytes (10), as confirmed in the present study by in situ hybridization (data not shown), we next investigated whether *Pol* $\lambda^{-/-}$ mice show infertility. Each of the six *Pol* $\lambda^{-/-}$ males, which survived for 9 to 15 weeks after birth, was housed with two wild-type female mice, which were monitored for 30 days for pregnancy. Although all of the *Pol* $\lambda^{-/-}$ males triggered vaginal plug formation in the female mice, no pregnancy was detected, indicating that *Pol* $\lambda^{-/-}$ males are sterile as a result of a defect in sperm function rather than impaired sexual behavior. The fertility of male *Pol* $\lambda^{+/-}$ and female *Pol* $\lambda^{-/-}$ mice was unaffected.

To determine whether spermatogenesis is impaired in *Pol* $\lambda^{-/-}$ males, we examined the contents of the cauda epididymis from *Pol* $\lambda^{-/-}$ and age-matched *Pol* $\lambda^{+/+}$ and *Pol* $\lambda^{+/-}$ male mice. In contrast to *Pol* $\lambda^{+/+}$ (Fig. *4A*) and *Pol* $\lambda^{+/-}$ mice (data not shown), spermatozoa with truncated tails and abnormally shaped heads were observed in the cauda epididymis of adult *Pol* $\lambda^{-/-}$ mice (Fig. 4B). These abnormal spermatozoa exhibited no motility (Fig. 4C).

Histological analysis revealed that the number and the size of seminiferous tubules did not differ between *Pol* $\lambda^{-/-}$ mice

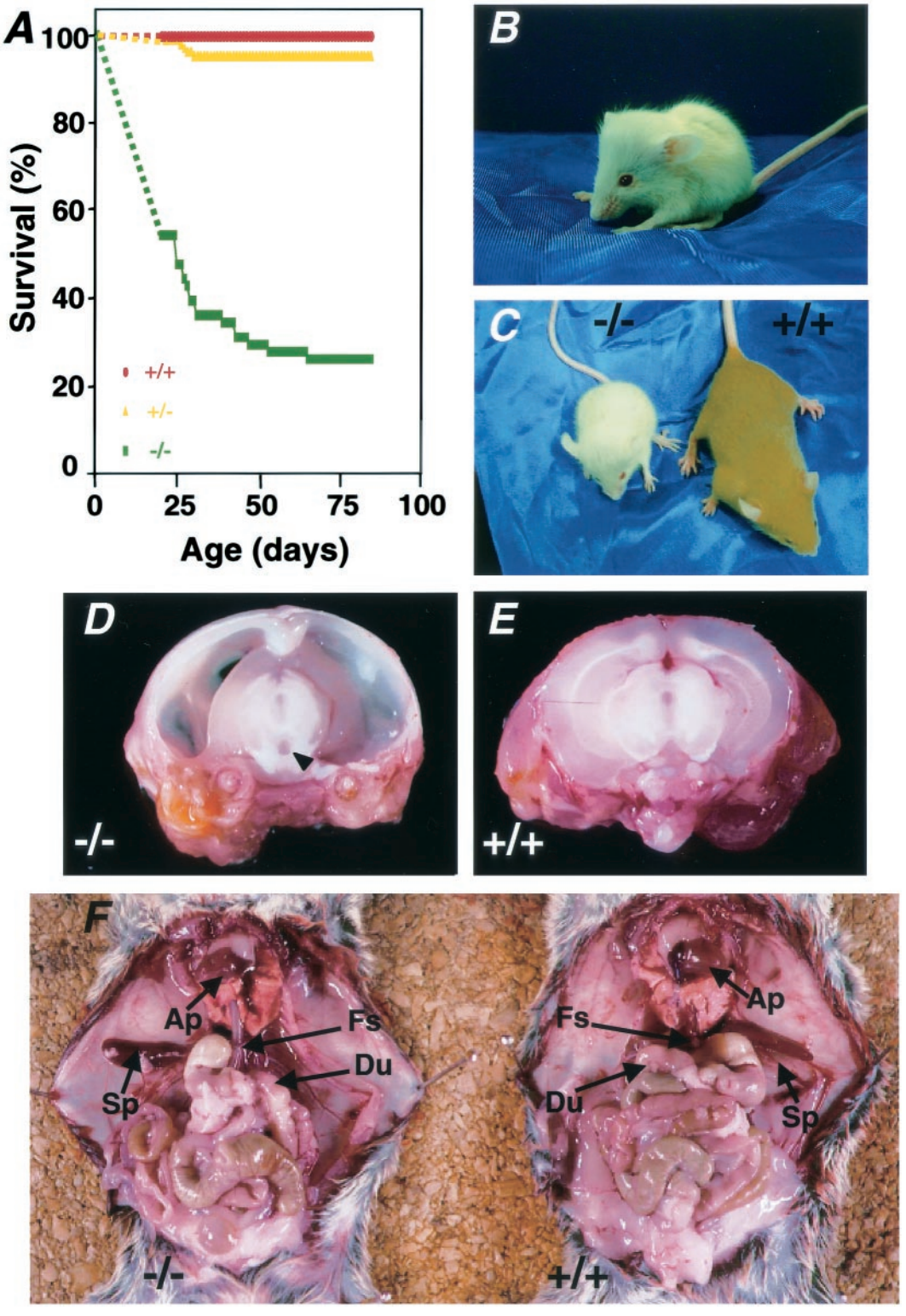

FIG. 2. Increased mortality, growth retardation, hydrocephalus, and situs inversus totalis in *Pol* $\lambda^{-/-}$ mice. (A) Survival rates of *Pol* $\lambda^{-/-}$, *Pol* $\lambda^{+/-}$, and *Pol* $\lambda^{+/+}$ mice (from strains 96 and 97) from 21 days of age after birth. The survival curves from birth to 21 days were shown as a dotted line, because exact survivals were not determined. The percentage of survival of *Pol* $\lambda^{-/-}$ mice at 21 days (58%) was estimated from the ratio of *Pol* $\lambda^{+/+}$, *Pol* $\lambda^{+/-}$, and *Pol* $\lambda^{-/-}$ animals (157:341:91) at 21 days. All *Pol* $\lambda^{-/-}$ mice were confirmed to have hydrocephalus at autopsy. (B) A *Pol* $\lambda^{-/-}$ mouse at 4 weeks of age with a dome-shaped head. (C) A 4-week-old *Pol* $\lambda^{-/-}$ mouse (left) exhibiting hydrocephalus and marked growth retardation compared with a wild-type littermate (right). (D and E) Sagittal sections of brains from *Pol* $\lambda^{-/-}$ mice (D) and wild-type littermates (E) at 5 weeks of age. Markedly enlarged lateral ventricles and a moderately dilated third ventricle (arrowhead) in *Pol* $\lambda^{-/-}$ mice were observed. (F) Situs inversus totalis with reversal of the abdominal organs, heart, lungs, and aorta after removal of the liver in *Pol* $\lambda^{-/-}$ (left) and *Pol* $\lambda^{+/+}$ (right) mice. AP, apex of the heart; Sp, spleen; Fs, forestomach; Du, duodenum.

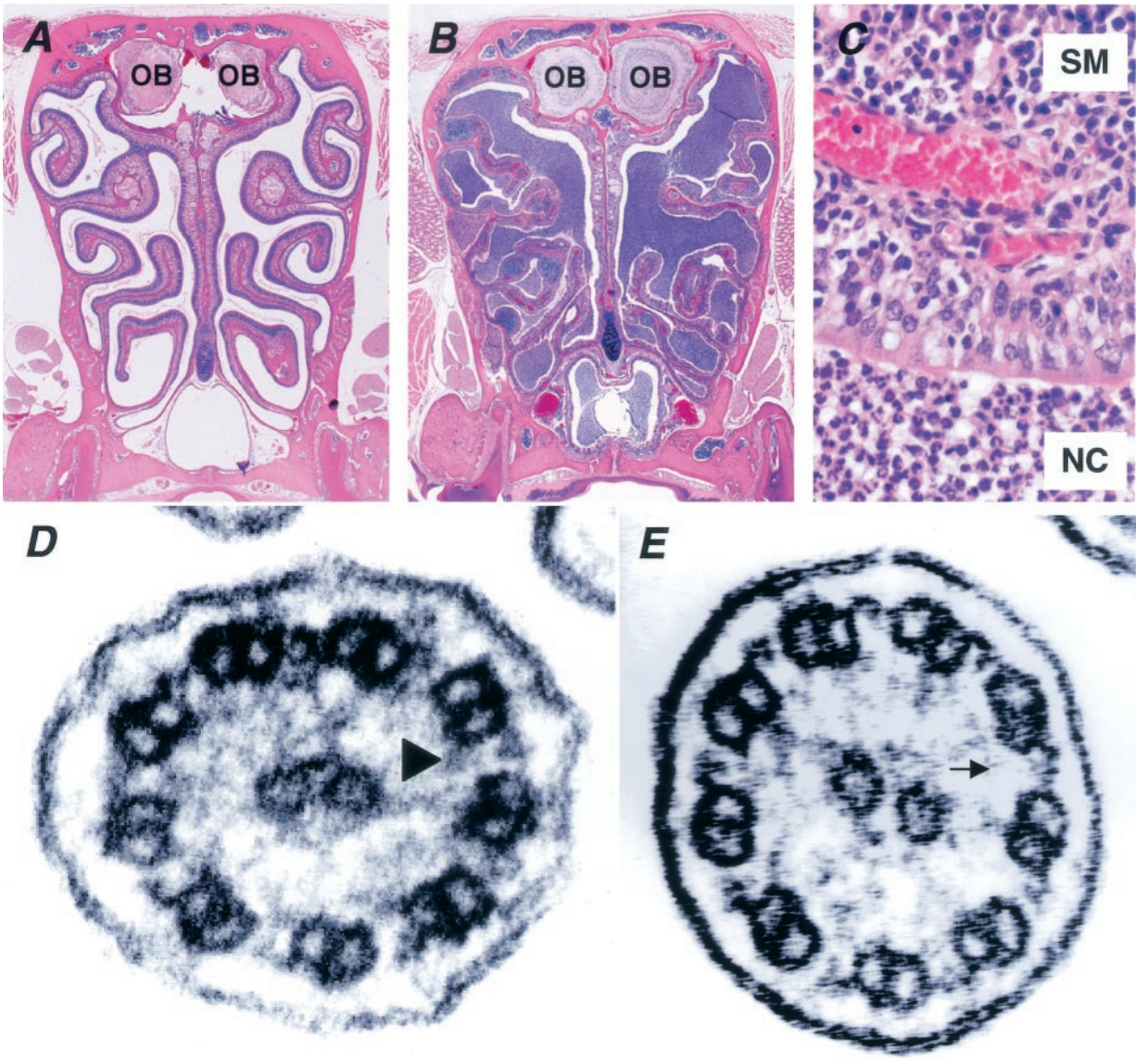

FIG. 3. Microscopic examination of paranasal cavity and ultrastructural analysis of the cilia from *Pol* $\lambda^{-/-}$ mice. Compared with wild-type littermates (A), marked infiltration of inflammatory cells was recognized in the paranasal sinuses of *Pol* $\lambda^{-/-}$ mice (B). OB, olfactory bulb. (C) A higher magnification of the paranasal sinuses of *Pol* $\lambda^{-/-}$ mice, showing accumulation of polymorphonuclear leukocytes in the nasal cavity (NC) and inflammatory cell infiltration mainly composed of plasma cells and angiogenesis in the submucosal regions (SM) of tunica mucosa olfactoria. (D and E) Electron micrographs of the respiratory epithelial cilia of wild-type (D) and *Pol* $\lambda^{-/-}$ (E) mice are shown. Wild-type cilia adopt a 9 + 2 microtubule arrangement with two dynein arms (outer and inner) (arrowhead), whereas the inner dynein arms are absent in the cilia from *Pol* $\lambda^{-/-}$ mice (arrow).

and their wild-type littermates aged 5 to 15 weeks (Fig. 4D and E). In mice, spermatogenesis can be classified into 16 steps (28). There was no histological abnormality in the pachytene cells and spermatogenesis in *Pol* $\lambda^{-/-}$ mice until step 12 was reached. At step 13, wild-type mice had spermatids with long tails protruding into the lumens of the seminiferous tubules and their heads lined up on the surface of seminiferous epithelia, while *Pol* $\lambda^{-/-}$ mice had spermatids with short tails, which were scattered over the lumens of seminiferous tubules (Fig. 4F and G). The epididymis of *Pol* $\lambda^{+/+}$ mice was filled with mature sperm with elongated tails, whereas in the epididymis of *Pol* $\lambda^{-/-}$ mice mature sperm were rarely recognized, and abnormal spermatozoa and residual body-like eosinophilic substances were observed (Fig. 4H and I). Importantly, microinjection of sperm from *Pol* $\lambda^{-/-}$ mice into oocytes gave rise to normal offspring, indicating that Pol λ-deficient sperm were genetically intact. These observations suggest that the meiotic recombination step in the maturation process of spermatids is normal in *Pol* $\lambda^{-/-}$ mice and that defective elongation of the tails of spermatids is responsible for the sterility of *Pol* $\lambda^{-/-}$ mice.

Pol λ is dispensable for cell growth and DNA damage repair. The rate of proliferation and morphology of *Pol* $\lambda^{-/-}$ ES cells were indistinguishable from those of Pol $\lambda^{+/+}$ and *Pol* $\lambda^{+/-}$ ES cells (data not shown). To evaluate the role of Pol λ in DNA repair, we examined the sensitivity of *Pol* $\lambda^{-/-}$ ES cells

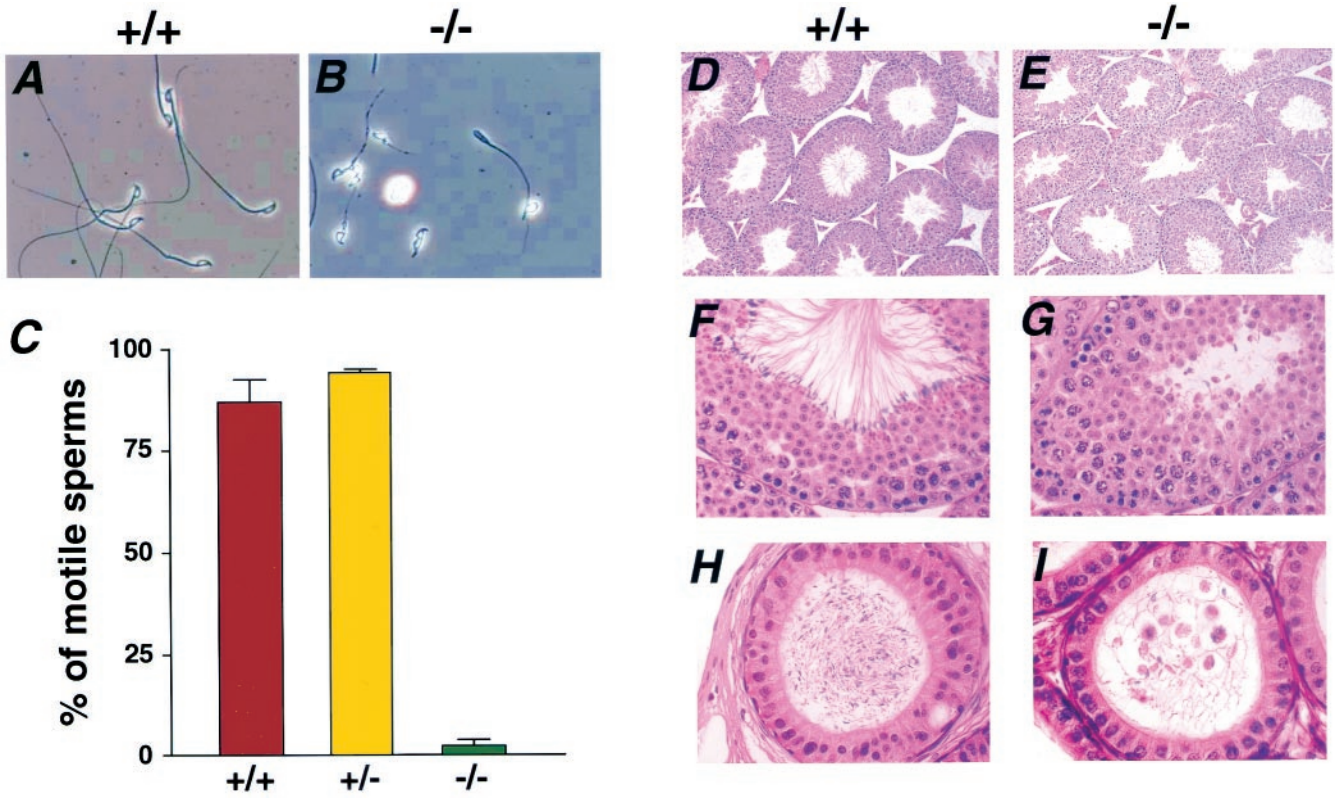

FIG. 4. Abnormal morphology and motility of sperm from *Pol* $\lambda^{-/-}$ mice. (A and B) Analysis of the contents of the cauda epididymis of wild-type (A) and *Pol* $\lambda^{-/-}$ (B) mice at 9 weeks of age. Sperm of *Pol* $\lambda^{-/-}$ mice exhibited shorter and snaggy tails and round-shaped heads. (C) Frequency of motile sperm from *Pol* $\lambda^{+/+}$, *Pol* $\lambda^{+/-}$, and *Pol* $\lambda^{-/-}$ mice. (D through G) Histological analysis of seminiferous tubules of 5-week-old wild-type (D and F) and *Pol* $\lambda^{-/-}$ (E and G) mice at low (D and E) and higher (F and G) magnification at stage VIII. No mature spermatids were seen at stage VIII in *Pol* $\lambda^{-/-}$ mice (G). (H and I) Histological analysis of the corpus epididymis of wild-type (H) and *Pol* $\lambda^{-/-}$ (I) mice at 7 weeks of age. The epididymis of *Pol* $\lambda^{-/-}$ mice contains immature sperm with snaggy tails, residual bodies, and basophilic monocuclear cells in the lumen (I).

to X-ray irradiation (Fig. 5A), UV irradiation (Fig. 5B), hydrogen peroxide (Fig. 5C), and MMS (Fig. 5D). DNA lesions generated by these reagents are mainly repaired by homologous recombination or nonhomologous end joining (for X-ray irradiation), nucleotide excision repair (for UV irradiation), and BER (for H_2O_2 and MMS), respectively. The sensitivity of *Pol* $\lambda^{-/-}$ ES cells to all DNA-damaging agents used in this study was indistinguishable from that of *Pol* $\lambda^{+/+}$ and *Pol* $\lambda^{+/-}$ ES cells (Fig. 5A through D), suggesting that Pol λ is not essential for the repair of damaged DNA.

DISCUSSION

The present study shows that *Pol* $\lambda^{-/-}$ mice develop pathological changes in the central nervous system, the paranasal sinuses, and the seminiferous tubules of the testis and nonrandom determinations of left-right asymmetry. These pathological changes are the hallmarks of immotile cilia syndrome, the essential feature of which is abnormal structure and function of cilia, consisting of nine microtubular doublets in a ring around two single microtubules (1). These 11 units are joined by three types of bonds, including two rows of dynein arms along each doublet, nexin links, and spokes. The immotile cilia syndrome is characterized by heterogeneous phenotypes and has been classified into several subgroups based on the status of the dynein arms, spoke defect, microtubular transposition defect, and disorganized axoneme. We have shown that the inner dynein arms of cilia from the respiratory epithelium and ependymal cell layer are defective in *Pol* $\lambda^{-/-}$ mice (Fig. 3E). Cilia with no outer dynein arms are capable of beating slowly, whereas the inner arms seem to be indispensable for ciliary movement (15, 33). Thus, it is suggested that cilia in *Pol* $\lambda^{-/-}$ mice are immotile due to a lack of inner dynein arms, which underlies the development of immotile cilia syndrome. As Pol λ has a BRCT motif at the N-terminal region, which is thought to mediate protein-protein interaction (34), it is possible that Pol λ interacts with a component(s) of cilia through the BRCT motif, thereby playing an essential role in cilia formation. Alternatively, Pol λ may interact with an unidentified protein(s) involved in transcription and chromatin structure and thereby modulate the transcription of a gene(s) for cilia formation.

Pol λ belongs to Pol X family of DNA polymerases and possesses DNA polymerase activity like Pol β, suggesting that it participates in BER (2, 10, 21). Although Pol β is crucial for short-patch BER of lesions generated by monofunctional alkylating agents such as MMS (30), it has been reported that a certain short-patch BER can be observed in Pol β-deficient cells (6, 31), suggesting that some other DNA polymerase(s) exists in mammalian cells that are involved in short-patch BER processes.

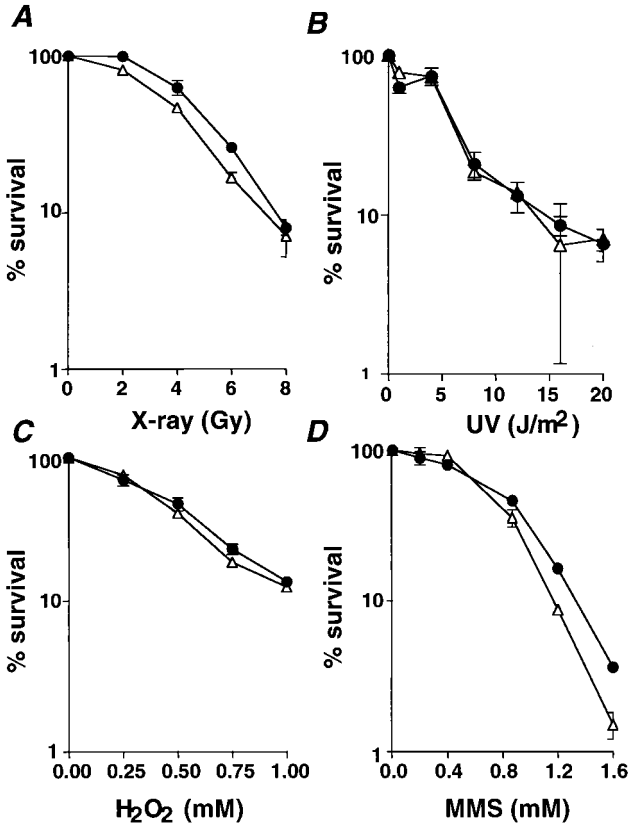

FIG. 5. Effect of various DNA-damaging agents on the survival of *Pol* $\lambda^{-/-}$ ES cells. Clonogenic survival of *Pol* $\lambda^{+/+}$ (solid circles) and *Pol* $\lambda^{-/-}$ ES cells (open triangles) after treatment with increasing doses of X-rays (A), UV irradiation (B), H_2O_2 (C), and MMS (D) is shown. All experiments were performed in triplicate. Consistent results were obtained in different sets of experiments. Data are presented as mean survival rates ± the standard deviation.

Pol λ possesses a 5′-deoxyribose-5-phosphate lyase activity in addition to DNA polymerase activity, although Pol λ is less potent than Pol β in these activities (9, 21). These features suggested that Pol λ is involved in BER of lesions generated by monofunctional alkylating agents. However, we could not observe any difference in sensitivity to DNA-damaging agents between *Pol* $\lambda^{-/-}$ ES cells and *Pol* $\lambda^{+/+}$ ES cells, including X-ray irradiation, UV irradiation, hydrogen peroxide, and MMS. These findings raise the possibility that Pol β, Pol δ, and Pol ε or some other DNA polymerase(s) compensates for the deficiency of Pol λ in short-patch and/or long-patch BER processes. Pol λ is highly expressed in the testis, especially in late pachytene spermatocytes (10, 21), suggesting that Pol λ participates in a meiotic recombination process and/or in DNA repair in spermatogenic cells. Male *Pol* $\lambda^{-/-}$ mice show impaired spermatogenesis and infertility, and the spermatozoa from *Pol* $\lambda^{-/-}$ mice are immotile but able to generate offspring by direct injection into oocytes. These results indicate that the meiotic recombination process and DNA repair are intact in *Pol* $\lambda^{-/-}$ mice and that Pol λ is dispensable for these processes during spermatogenesis. The detailed function of Pol λ in DNA repair remains to be elucidated.

In this study, we have established *Pol* $\lambda^{-/-}$ mice, which may provide a suitable model for investigating the pathogenesis of immotile cilia syndrome.

ACKNOWLEDGMENTS

We thank Y. Nishimune, S. Torigai, K. Watanabe, and W. W. Hall for their helpful suggestions and discussions; Y. Orba and M. Satoh for histological analysis; T. Iwata for spermatozoa analysis; and Y. Eto and K. Tsutsumi for technical assistance.

This study was supported in part by Health Science Research Grants for Comprehensive Research on Aging and Health (H11-chouju-005 to N.M.) and for Human Genome and Gene Therapy (H10-genomu-001 to K.I.) from the Ministry of Health and Welfare of Japan. Y.O. is a research fellow of the Japan Society for the Promotion of Science.

Y.K., M.W., and Y.O. contributed equally to this work.

REFERENCES

1. **Afzelius, B. A., and B. Mossberg.** 1995. Immotile-cilia syndrome (primary ciliary dyskinesia), including Kartagener syndrome, p. 3943–3954. *In* C. R. Scriber, A. L. Beaudet, W. S. Sly, and D. Valle (ed.), The metabolic and molecular bases of inherited disease, vol. 3. McGraw-Hill, Inc., New York, N.Y.
2. **Aoufouchi, S., E. Flatter, A. Dahan, A. Faili, B. Bertocci, S. Storck, F. Delbos, L. Cocea, N. Gupta, J. C. Weill, and C. A. Reynaud.** 2000. Two novel human and mouse DNA polymerases of the polX family. Nucleic Acids Res. **28:**3684–3693.
3. **Bork, P., K. Hofmann, P. Bucher, A. F. Neuwald, S. F. Altschul, and E. V. Koonin.** 1997. A superfamily of conserved domains in DNA damage-responsive cell cycle checkpoint proteins. FASEB J. **11:**68–76.
4. **Callebaut, I., and J. P. Mornon.** 1997. From BRCA1 to RAP1: a widespread BRCT module closely associated with DNA repair. FEBS Lett. **400:**25–30.
5. **Dianov, G. L., R. Prasad, S. H. Wilson, and V. A. Bohr.** 1999. Role of DNA polymerase beta in the excision step of long patch mammalian base excision repair. J. Biol. Chem. **274:**13741–13743.
6. **Fortini, P., B. Pascucci, E. Parlanti, R. W. Sobol, S. H. Wilson, and E. Dogliotti.** 1998. Different DNA polymerases are involved in the short- and long-patch base excision repair in mammalian cells. Biochemistry **37:**3575–3580.
7. **Friedberg, E. C., W. J. Feaver, and V. L. Gerlach.** 2000. The many faces of DNA polymerases: strategies for mutagenesis and for mutational avoidance. Proc. Natl. Acad. Sci. USA **97:**5681–5683.
8. **Frosina, G., P. Fortini, O. Rossi, F. Carrozzino, G. Raspaglio, L. S. Cox, D. P. Lane, A. Abbondandolo, and E. Dogliotti.** 1996. Two pathways for base excision repair in mammalian cells. J. Biol. Chem. **271:**9573–9578.
9. **Garcia-Diaz, M., K. Bebenek, T. A. Kunkel, and L. Blanco.** 2001. Identification of an intrinsic 5′-deoxyribose-5-phosphate lyase activity in human DNA polymerase lambda: a possible role in base excision repair. J. Biol. Chem. **276:**34659–34663.
10. **Garcia-Diaz, M., O. Dominguez, L. A. Lopez-Fernandez, L. T. de Lera, M. L. Saniger, J. F. Ruiz, M. Parraga, M. J. Garcia-Ortiz, T. Kirchhoff, J. del Mazo, A. Bernad, and L. Blanco.** 2000. DNA polymerase lambda (Pol lambda), a novel eukaryotic DNA polymerase with a potential role in meiosis. J. Mol. Biol. **301:**851–867.
11. **Gavrieli, Y., Y. Sherman, and S. A. Ben-Sasson.** 1992. Identification of programmed cell death in situ via specific labeling of nuclear DNA fragmentation. J. Cell Biol. **119:**493–501.
12. **Goodman, M. F., and B. Tippin.** 2000. The expanding polymerase universe. Nat. Rev. Mol. Cell Biol. **1:**101–109.
13. **Horton, J. K., D. K. Srivastava, B. Z. Zmudzka, and S. H. Wilson.** 1995. Strategic down-regulation of DNA polymerase beta by antisense RNA sensitizes mammalian cells to specific DNA damaging agents. Nucleic Acids Res. **23:**3810–3815.
14. **Hubscher, U., H. P. Nasheuer, and J. E. Syvaoja.** 2000. Eukaryotic DNA polymerases, a growing family. Trends Biochem. Sci. **25:**143–147.
15. **Kamiya, R., and M. Okamoto.** 1985. A mutant of *Chlamydomonas reinhardtii* that lacks the flagellar outer dynein arm but can swim. J. Cell Sci. **74:**181–191.
16. **Kawase, Y., T. Iwata, Y. Toyoda, T. Wakayama, R. Yanagimachi, and H. Suzuki.** 2001. Comparison of intracytoplasmic sperm injection for inbred and hybrid mice. Mol. Reprod. Dev. **60:**74–78.
17. **Kawase, Y., T. Iwata, M. Watanabe, N. Kamada, O. Ueda, and H. Suzuki.** 2001. Application of the piezo-micromanipulator for injection of embryonic stem cells into mouse blastocysts. Contemp. Top. Lab. Anim. Sci. **40:**31–34.
18. **Matsumoto, Y., and K. Kim.** 1995. Excision of deoxyribose phosphate residues by DNA polymerase beta during DNA repair. Science **269:**699–702.
19. **Matsumoto, Y., K. Kim, and D. F. Bogenhagen.** 1994. Proliferating cell nuclear antigen-dependent abasic site repair in *Xenopus laevis* oocytes: an alternative pathway of base excision DNA repair. Mol. Cell. Biol. **14:**6187–6197.

20. **Motoyama, N., F. Wang, K. A. Roth, H. Sawa, K. Nakayama, I. Negishi, S. Senju, Q. Zhang, S. Fujii, et al.** 1995. Massive cell death of immature hematopoietic cells and neurons in Bcl-x-deficient mice. Science **267:**1506–1510.
21. **Nagasawa, K., K. Kitamura, A. Yasui, Y. Nimura, K. Ikeda, M. Hirai, A. Matsukage, and M. Nakanishi.** 2000. Identification and characterization of human DNA polymerase beta 2, a DNA polymerase beta-related enzyme. J. Biol. Chem. **275:**31233–31238.
22. **Nealon, K., I. D. Nicholl, and M. K. Kenny.** 1996. Characterization of the DNA polymerase requirement of human base excision repair. Nucleic Acids Res. **24:**3763–3770.
23. **Ochs, K., R. W. Sobol, S. H. Wilson, and B. Kaina.** 1999. Cells deficient in DNA polymerase beta are hypersensitive to alkylating agent-induced apoptosis and chromosomal breakage. Cancer Res. **59:**1544–1551.
24. **Oda, N., J. K. Saxena, T. M. Jenkins, R. Prasad, S. H. Wilson, and E. J. Ackerman.** 1996. DNA polymerases alpha and beta are required for DNA repair in an efficient nuclear extract from *Xenopus* oocytes. J. Biol. Chem. **271:**13816–13820.
25. **Pelletier, H., M. R. Sawaya, A. Kumar, S. H. Wilson, and J. Kraut.** 1994. Structures of ternary complexes of rat DNA polymerase beta, a DNA template-primer, and ddCTP. Science **264:**1891–1903.
26. **Plug, A. W., C. A. Clairmont, E. Sapi, T. Ashley, and J. B. Sweasy.** 1997. Evidence for a role for DNA polymerase beta in mammalian meiosis. Proc. Natl. Acad. Sci. USA **94:**1327–1331.
27. **Podlutsky, A. J., I. I. Dianova, V. N. Podust, V. A. Bohr, and G. L. Dianov.** 2001. Human DNA polymerase beta initiates DNA synthesis during long-patch repair of reduced AP sites in DNA. EMBO J. **20:**1477–1482.
28. **Russell, L. D., R. A. Ettlin, A. P. Sinha Hikim, and E. D. Clegg.** 1990. Histological and histopathological evaluation of the testis. Cache River Press, Clearwater, Fla.
29. **Sobol, R. W., J. K. Horton, R. Kuhn, H. Gu, R. K. Singhal, R. Prasad, K. Rajewsky, and S. H. Wilson.** 1996. Requirement of mammalian DNA polymerase-beta in base-excision repair. Nature **379:**183–186.
30. **Sobol, R. W., R. Prasad, A. Evenski, A. Baker, X. P. Yang, J. K. Horton, and S. H. Wilson.** 2000. The lyase activity of the DNA repair protein beta-polymerase protects from DNA-damage-induced cytotoxicity. Nature **405:**807–810.
31. **Stucki, M., B. Pascucci, E. Parlanti, P. Fortini, S. H. Wilson, U. Hubscher, and E. Dogliotti.** 1998. Mammalian base excision repair by DNA polymerases delta and epsilon. Oncogene **17:**835–843.
32. **Tybulewicz, V. L., C. E. Crawford, P. K. Jackson, R. T. Bronson, and R. C. Mulligan.** 1991. Neonatal lethality and lymphopenia in mice with a homozygous disruption of the c-abl proto-oncogene. Cell **65:**1153–1163.
33. **Weaver, A., and R. Hard.** 1985. Isolation of newt lung ciliated cell models: characterization of motility and coordination thresholds. Cell Motil. **5:**355–375.
34. **Zhang, X., S. Morera, P. A. Bates, P. C. Whitehead, A. I. Coffer, K. Hainbucher, R. A. Nash, M. J. Sternberg, T. Lindahl, and P. S. Freemont.** 1998. Structure of an XRCC1 BRCT domain: a new protein-protein interaction module. EMBO J. **17:**6404–6411.